



## In situ laboratory sea spray production during the Marine Aerosol Production 2006 cruise on the northeastern Atlantic Ocean

Kim A. H. Hultin,<sup>1</sup> E. Douglas Nilsson,<sup>1</sup> Radovan Krejci,<sup>1</sup> E. Monica Mårtensson,<sup>1</sup> Mikael Ehn,<sup>2</sup> Åke Hagström,<sup>3</sup> and Gerrit de Leeuw<sup>4,5</sup>

Received 20 May 2009; revised 13 October 2009; accepted 20 October 2009; published 17 March 2010.

[1] Bubbles bursting from whitecaps are considered to be the most effective mechanism for particulate matter to be ejected into the atmosphere from the Earth's oceans. To realistically predict the climate effect of marine aerosols, global climate models require process-based understanding of particle formation from bubble bursting. During a cruise on the highly biologically active waters of the northeastern Atlantic Ocean in the summer of 2006, the submicrometer primary marine aerosol produced by a jet of seawater impinging on a seawater surface was investigated. The produced aerosol size spectra were centered on 200 nm in dry diameter and were conservative in shape throughout the cruise. The aerosol number production was negatively correlated with dissolved oxygen (DO) in the water ( $r < -0.6$  for particles of dry diameter  $D_p > 200$  nm). An increased surfactant concentration as a result of biological activity affecting the oxygen saturation is thought to diminish the particle production. The lack of influence of chlorophyll on aerosol production indicates that hydrocarbons produced directly by the photosynthesis are not essential for sea spray production. The upward mixing of deeper ocean water as a result of higher wind speed appears to affect the aerosol particle production, making wind speed influence aerosol production in more ways than by increasing the amount of whitecaps. The bubble spectra produced by the jet of seawater was representative of breaking waves at open sea, and the particle number production was positively correlated with increasing bubble number concentration with a peak production of 40–50 particles per bubble.

**Citation:** Hultin, K. A. H., E. D. Nilsson, R. Krejci, E. M. Mårtensson, M. Ehn, Å. Hagström, and G. de Leeuw (2010), In situ laboratory sea spray production during the Marine Aerosol Production 2006 cruise on the northeastern Atlantic Ocean, *J. Geophys. Res.*, 115, D06201, doi:10.1029/2009JD012522.

### 1. Introduction

[2] Aerosols play a significant role in the Earth's radiative budget, where their major influence on our climate is through their role as cloud condensation nuclei (CCN) and as ice nuclei (IN), an influence not yet satisfactory estimated [Intergovernmental Panel on Climate Change (IPCC), 2007]. Increase in the CCN concentration causes an increase in cloud droplet number concentration, which enhances cloud albedo. With more aerosol particles and the same amount of water in the clouds, the cloud droplet radius will decrease, resulting in a decrease in the precipitation efficiency and increased cloud lifetime. Both these effects caused by the aerosols lead to a climate cooling.

[3] Marine aerosols in particular are of high interest since about 70% of the Earth's surface is covered by oceans, and marine aerosols hence are representative of a significant fraction of aerosols found in the atmosphere (see Seinfeld and Pandis [2006] for the production on an annual basis). Aerosol constituents can be separated into two types: primary and secondary aerosols, where the former is directly injected into the atmosphere from the Earth's surface, and the latter is formed mainly by gas-to-particle conversion processes in the atmosphere. The major source of primary marine aerosol particles is the bursting of bubbles on the ocean surface [Blanchard, 1983]. The bubbles originate from breaking waves caused by wind drag on the ocean surface. Breaking waves entrain air into the ocean surface water, which breaks up into bubbles. The bubbles subsequently rise to the surface under the influence of their buoyancy, where they burst and eject small droplets into the air. This results in a wind-driven source of aerosol particles [O'Dowd *et al.*, 1997; Nilsson *et al.*, 2001]. The surface manifestation of a bubble plume is a whitecap, which can be parameterized as a function of environmental parameters such as wind speed, atmospheric thermal stability, and water temperature [Monahan and O'Muircheartaigh, 1986].

<sup>1</sup>Department of Applied Environmental Science, Stockholm University, Stockholm, Sweden.

<sup>2</sup>Department of Physics, University of Helsinki, Helsinki, Finland.

<sup>3</sup>Swedish Institute for the Marine Environment, Gothenburg, Sweden.

<sup>4</sup>TNO Built Environmental and Geosciences, Utrecht, Netherlands.

<sup>5</sup>Now at Climate Change Unit, Finnish Meteorological Institute, Helsinki, Finland.

[4] While bubbles rise to the surface, surface active material in the bulk water aggregates to the walls of the bubbles. This material consists mainly of organic chemicals of either natural or anthropogenic origin. Usually, the cause of their surface activity is that individual molecules contain both hydrophobic and hydrophilic moieties, causing these substances to accumulate at an air-water interface such as the ocean surface or on bubbles or droplets. The organic chemicals arise from within the water body, or from materials carried to the water surface by winds, air currents, and precipitation [Wotton and Preston, 2005]. The result is lowered surface tension, possibly affecting interfacial mass transport and other surface properties [Lewis and Schwartz, 2004]. When reaching the water-air interface, the bubbles are enriched with organic surfactants and/or microorganisms that accumulate there. Once the bubbles burst at the ocean surface, the gathered material concentrated on the walls is injected into the atmosphere.

[5] When a bubble reaches the surface, disrupting the surface film of the water, the bubble breaks up into many so-called film droplets. After bursting of the bubble film, so-called jet droplets are formed from the vertically rising jet of water from the collapsing bubble cavity. Compared to film droplets, the number of jet droplets is small, and their size is generally larger. While aerosol from jet droplets is mainly found in the supermicrometer size range, the submicrometer aerosol is the result of film droplets [Cipriano and Blanchard, 1981; Afeti and Resch, 1990; Reinke et al., 2001]. The bubbles producing film drops are expected to be rather large; these should primarily be formed from bubbles that are larger than 2–2.5 mm [Blanchard and Syzdek, 1988; Resch and Afeti, 1992]. The material reaching the atmosphere as aerosols consists of a mixture of sea salt, organic matter [Blanchard and Syzdek, 1982; Cavalli et al., 2004], and even marine bacteria [Blanchard and Syzdek, 1982; Marks et al., 2001].

[6] Until a decade ago, primary marine aerosol studies were mainly focused on supermicron aerosol particles because of their effect on atmospheric transmission and the sea-air transfer of heat and water vapor [e.g., Andreas, 1998], for which aerosol mass is a key parameter. Primary marine aerosol has also been recognized as important for many aspects of atmospheric chemistry [e.g., Gong et al., 1997a, 1997b; von Glasow and Crutzen, 2004]. With the realization of the role aerosols play in the climate of the Earth [Charlson et al., 1992], focus has shifted in the last decade to studies of sea spray submicron particles over the size range from roughly 10 nm to 1  $\mu\text{m}$  [Gong, 2003]. This size range is important for, for example, the direct radiative effect and cloud formation. In the submicrometer size range, sea salt is also the prime Mie-scatterer in remote marine areas, larger than the marine biogenic sulphate [Murphy et al., 1998]. The number and size of particles, as mentioned before, relates to the cloud albedo, and aerosols in the accumulation mode form the majority of CCN [O'Dowd et al., 1997]. As the measuring techniques developed, more experiments have been conducted regarding submicrometer aerosol particles.

[7] Global climate models predict future changes in surface water temperature, wind speed, and sea ice cover, all parameters with potential climate feedback through their

effects on sea spray production [Nilsson et al., 2001]. The global climate models require process-based understanding of particle formation from bubble bursting. The challenge in understanding this type of particle formation begins with the variability of the atmospheric environment, where controlled laboratory experiments are essential for isolating the effects of a limited number of parameters.

[8] Laboratory work performed by Mårtensson et al. [2003] indirectly suggests seasonal and geographical differences in the production of primary marine aerosols, where the number of particles produced depends on the water temperature and varies with particle size. When Pierce and Adams [2006] applied the Mårtensson et al. [2003] parameterization in a global model, it was demonstrated that the temperature dependency has important regional effects. Mårtensson et al. [2003] also indicate that droplet formation is affected by salinity. Fieldwork on the North Atlantic has shown that both the physical and chemical properties of the marine aerosol exhibited clear seasonal patterns following the biological activity in water [O'Dowd et al., 2004; Sellegri et al., 2006; Yoon et al., 2007].

[9] The present study investigates the aerosol production from the bubble-bursting mechanism, using fresh oceanic water directly sampled in an algae bloom, during a ship campaign at open sea. We explore the microphysical characteristics of sea spray, with respect to the influence of such variables as water temperature and dissolved oxygen, but also investigate the influence of biological activity in the water and the effect of different meteorological conditions. In particular, we focus on size spectra for particles smaller than those which can be measured with optical particle counters (OPCs), since the size resolved production in this range cannot be determined using the eddy covariance method [cf. Nilsson et al., 2007]. There have been several previous studies of the aerosol produced from real or artificial water with artificial entrainment of air to form bubbles. Most of them focused on the supermicrometer aerosol, however [e.g., Cipriano and Blanchard, 1981; Afeti and Resch, 1990; Stramska et al., 1990], and only recently have experiments included the submicrometer size range [Mårtensson et al., 2003; Sellegri et al., 2006; Tyree et al., 2007]. Only in one case was real seawater used [Keene et al., 2007]. In comparison, our results represent the summer biologically highly productive northeastern Atlantic, compared to water representative of the less productive Sargasso Sea in the work of Keene et al. [2007].

## 2. Methods and Location

[10] This study is part of the EU project Marine Aerosol Production from Natural Sources (MAP), and data were sampled continuously during a cruise on the northeastern Atlantic west of Ireland with the Irish research vessel R/V *Celtic Explorer* from 11 June to 5 July in 2006 (see Figure 1). The cruise track was guided by the most productive areas determined from Moderate Resolution Imaging Spectroradiometer (MODIS) ocean color products as well as by onboard measurements of  $\text{CO}_2$  partial pressure and fluorescence in the seawater. The average chlorophyll  $a$  concentration during the MAP cruise was 1.4  $\mu\text{g L}^{-1}$ . The cruise was broken up by one port call. During the first

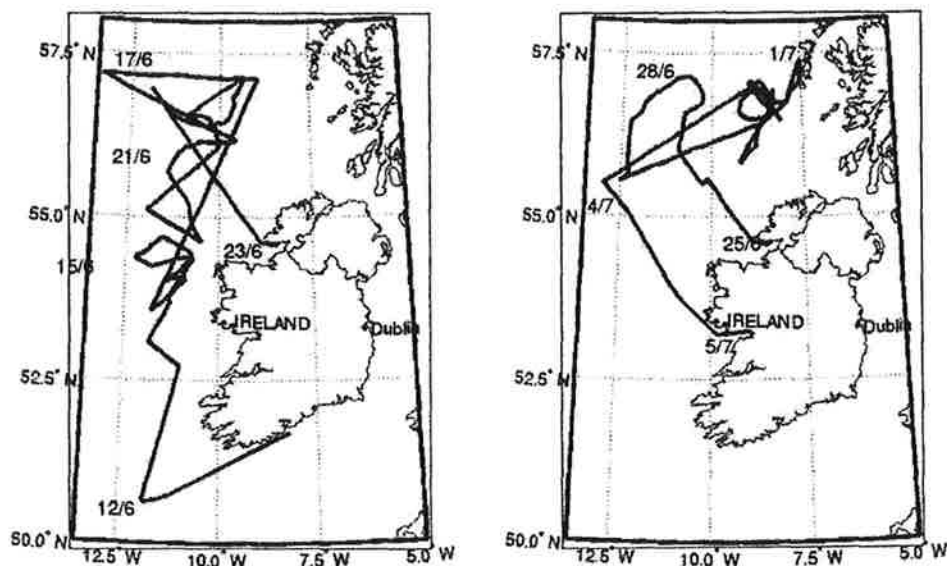


**Figure 1.** Ship track. Start, 11 June 2006 from Cobh (51.7°N, 8.24°E). Port call, 23–24 June 2006 at Killybegs (54.6°N, 8.48°E), and finish 5 July 2006 at Galway (53.2°N, 9.0°E).

leg, we encountered a storm with wind speed exceeding  $25 \text{ m s}^{-1}$ , while the second leg was characterized by low to moderate winds. The MAP expedition data represent open seawater with salinity of about 35 psu (practical salinity units) and high biological productivity.

### 2.1. Experimental Setup

[11] Water was sampled continuously through a water supply system with an inlet beneath the ship bow at about 2 m below mean sea surface. Water was continuously being pumped at a constant rate of  $3 \text{ L min}^{-1}$  into a carefully sealed polyethylene bottle filled with approximately 13 L of water. The water entered through the top of the bottle as a vertical jet of water hitting the surface below to simulate the air entrainment caused by a breaking wave (see Figure 2). The bubble plume extended about 15 cm down into the water, a modest depth considering that entrained air bubbles from breaking waves can reach depths of several meters in high wind speed [Thorpe, 1982]. It should be mentioned, however, that the majority of entrained air is located within approximately 50 cm from the sea surface [Lamarre and Melville, 1992]. In nature, a whitecap bubble spectrum is the result of the breakup of large volumes of air entrained in the water by breaking waves, where the quantity of air involved in the breakup may vary, the shape of the resultant bubble spectrum remains constant [Cipriano *et al.*, 1983]. The number of bubbles produced, and thus the resulting aerosol flux, depends on the intensity of wave breaking. In our experiments we simulate this process with the jet of seawater falling onto the water surface with the amount of water streaming into the tank and the height from which it falls determining the bubble spectra [Cipriano and Blanchard, 1981]. When using a frit or similar to produce bubbles, the resulting bubble spectrum depends on frit pore size and air flow rates, among other things. It is also possible that particles may be produced by shearing forces at the pores

[Cipriano *et al.*, 1983]. Further details about the bottle can be found in Table 1.

[12] The bottle was standing on a gimbaled table in order to limit any influence of ship motions on the bubble and aerosol formation. An air line was connected to the bottle to pump filtered, and thus particle-free, air into the bottle in excess (more air was pumped in than sampled, the excess air flow leaking out of the bottle was kept at about 1 bar) to ensure that no laboratory air entered the bottle. Regularly, the water jet was turned off to control that the air in the bottle returned to zero particles without the jet, before the water jet was turned on again.

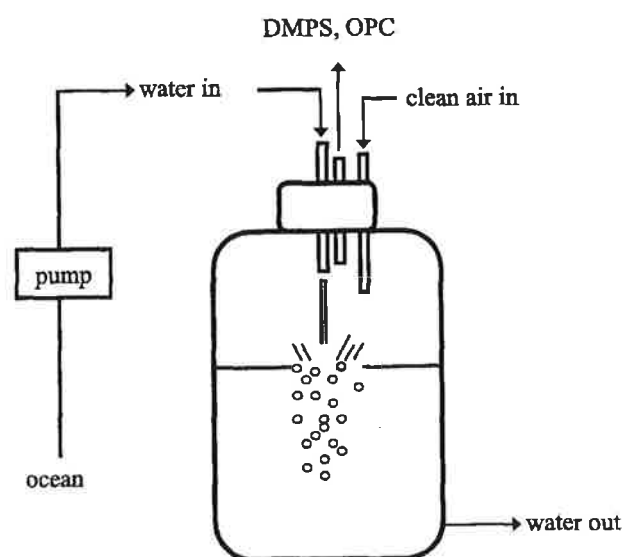


**Figure 2.** Schematic figure of the experiment tank. A jet of water simulates the action of a breaking wave. Water is continuously pumped from the North Atlantic into the tank.

**Table 1.** Characteristics of the Aerosol Generation Bottle

Characteristic	Value
Water inlet (m)	-2
Water flow rate (constant) ( $\text{min}^{-1}$ )	3
Water volume (L)	13
Head space volume (L)	7
Distance from nozzle to water surface (cm)	16
Extension of water plume into the water (cm)	15
Turnover time (min)	4

[13] The total number of aerosol particles produced was measured with a condensation particle counter (CPC), TSI model 3010. The aerosol size distribution created in the polyethylene bottle was measured with a differential mobility particle sizer (DMPS) and an OPC, together covering the size range between 0.02 and 2  $\mu\text{m}$  (dry diameter  $D_p$ ). The custom made DMPS system consisted of a differential mobility analyzer (DMA) operated with close loop sheath air [Jokinen and Mäkelä, 1997], delivering aerosol size distribution with  $D_p$  between 0.02 and 0.25  $\mu\text{m}$  in 15 bins together with a CPC (TSI 3010). The OPC (Grimm GmbH, model 7.309) measured the aerosol size distribution in 12 channels between 0.26 and 2.2  $\mu\text{m}$ . Half of the monodisperse aerosol passed through a thermodenuder, where the aerosol was heated to 300°C. The number of particles remaining after such high heating was analyzed using another DMA, a copy of the first one, and counted with a CPC (TSI 3010) with cutoff 0.006  $\mu\text{m}$  derived from laboratory calibration using ammonium sulfate. Total sample flow was constant at 6.3  $\text{L min}^{-1}$ , resulting in a scan through the particle sizes in 300 s, and a turn-over time of the air in the bottle of the order of 1 min. The length of the tubing used for sampling was less than 2 m, and thus diffusion losses are negligible. The losses by diffusion are overall very small for particles larger than 10 nm that we measured; the penetrating efficiency for 10 nm particles is 94%, while for 20 nm particles it is 97%. Losses by impaction become important well above our OPC measurement range as the whole setup has a size limitation around 4  $\mu\text{m}$ .

[14] Measuring both the size distributions for the total (dry) aerosol, and the aerosol remaining after heating to 300°C, it was initially our intention to interpret the later as the sea salt, and the difference as semivolatile, presumably organic compounds. Heating the aerosol to 300°C has so far been the established way to determine the sea-salt fraction of the aerosol; see, for example, O'Dowd and Smith [1993] and Brooks *et al.* [2002]. However, seawater contains compounds that do not evaporate when heated to only 300°C within the short contact time in a volatility system. Amino acids such as alanine, and fatty acids such as stearic and oleic acid all have boiling points near of or over 300° [Jarvis *et al.*, 1967; Kuznetsova *et al.*, 2005]. Unfortunately, no measurements were made during MAP to reveal the exact organic composition of the seawater. What is left after heating to 300°C will here be called "sea salt + nonvolatile organics," or SS + NVO.

[15] Water temperature, salinity, and dissolved oxygen were measured in the outflow water from the tank (Stratos 2402 Cond for temperature and salinity, Stratos 2402 Oxy for oxygen from Knick Elektronische Messgeräte GmbH and Company). Fluorescence was measured as a proxy for

chlorophyll  $\alpha$  on the same sampling line before the bubble tank as an indication of biological activity in the water. The fluorometer (Turner AU10, Turner Designs, USA) was calibrated against standards to check electronic integrity. Measurements made by the University of East Anglia of chlorophyll  $\alpha$  in the water ensured a good correlation (correlation coefficient  $r = 0.82$ , ship fluorometer =  $0.23 \times \text{chl } a + 0.01$ , number of paired data was 24) between fluorometer data and chlorophyll  $\alpha$ . We will from now on refer to the fluorescence as chlorophyll  $\alpha'$ . Dissolved organic carbon (DOC) in the water was determined by filtration of fresh seawater using quartz filters on board the ship, and analyzed using the methodology described by Facchini *et al.* [2008].

[16] Water from the sampling line was also led through three similar separate larger high-grade stainless steel tanks (55 cm in diameter, 1 m high). In these tanks, aerosols were produced in the same way, by letting a jet of constant seawater flow impinge on the seawater surface inside the tank. Subsurface bubble spectra in the size range from 30 to 1000  $\mu\text{m}$  were measured in one of the steel tanks, using the TNO optical bubble measuring system (well described by Leifer *et al.* [2003]). Compared with the aerosol generation tank, the flow of water used to produce the bubbles was low although the water jet height was similar (0.33  $\text{L min}^{-1}$  and 15 cm; see Table 1). The position for bubble measurement was about 4 cm below the water surface; however, the bubble plume depth is unknown. The TNO bubble system could not be submerged in a closed stainless steel tank, because it was too large and needed to be used in other experiments as well. Performing the physics experiments in an open tank would have resulted in contamination of the aerosol samples with particles from the dirty laboratory environment. Therefore the bubble measurements were conducted in a separate open stainless steel tank, and the water was continuously replaced in this tank from the same source. The other tanks were occupied with aerosol sampling for chemical analysis with methods requiring long sampling periods, which is the reason why they were kept separate from the physical measurements, in order to avoid contamination. These larger tanks were not compensated for ship motions. Data from these tanks will be published separately (starting with Facchini *et al.* [2008]). The current publication serves also the purpose of characterizing the physics of the produced aerosol for these publications.

## 2.2. Data Quality

[17] The sampling period suffered a fair share of problems, ranging from broken instruments caused by the storm encountered in the first leg, to technical problems with the SS + NVO measurements. As mentioned in section 2.1, the water jet was regularly turned off to check that the air in the bottle returned to zero particles without the jet to ensure that the measurements excluded all other aerosol sources except the bubble-bursting process. Even so, the SS + NVO aerosol measurements often exceeded the simultaneous total aerosol measurements in one or more size bin, often by as much as a factor of 10. The uncertainty in the particle number concentration measured by the CPCs depends on counting statistics or Poisson statistics. The standard deviation is given by the square root of the number of particles

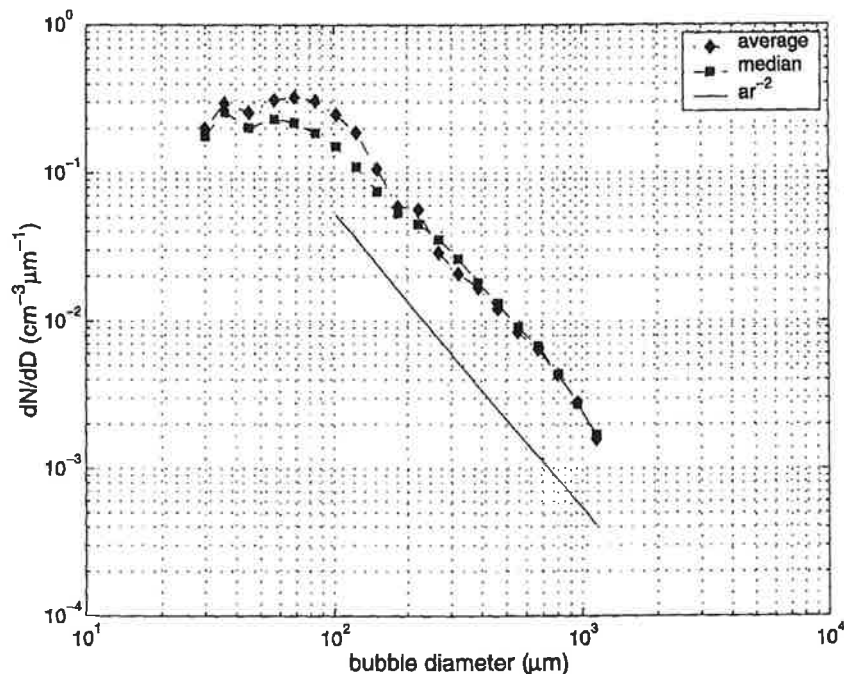


**Figure 3.** Average (diamonds and dash-dotted line) and median (circle and dashed line) bubble size distribution during the MAP cruise artificial sea spray experiments; number of scans  $N$  was 97. The solid line shows the parameterized bubble spectra using equation (1) with  $a = 270$  and  $b = 2$ .

counted during a sampling period. The Poisson errors for the CPCs are 1% for concentrations over  $100 \text{ cm}^{-3}$  and less than 3% for concentrations of about  $10 \text{ cm}^{-3}$  (10 s averages). All losses in the thermodenuder are corrected on the basis of scans comparing both size distributions with the heater turned off, and the thermophoretic velocity is calculated to be of the order of  $10^{-5}$  to  $10^{-4} \text{ m s}^{-1}$  (particle diameter  $>$  mean free path [Hinds, 1999; Baron and Willeke, 2005]). With other losses corrected for, and with such a low thermophoretic velocity compared with the sample flow, we therefore conclude that the SS + NVO aerosol is not the result of losses in the heating system, and that data containing heated number densities exceeding unheated ones do have a physical explanation.

[18] The SS + NVO increase could possibly result from pollution due to too much evaporated mass in the thermodenuder. The fraction of volatile aerosol mass gets deposited on the walls and at a certain point, it reaches a critical level and the evaporated mass starts to nucleate downstream of the thermodenuder where temperature drops rapidly. Another possibility is the fracture of sea-salt particles upon phase change when entering the thermodenuder (see Lewis and Schwartz [2004] for a summary on the subject). Since no satisfactory explanation was found to this behavior, and these occasions were evenly spread over the cruise and no correlation was found to any other parameter, all scans experiencing SS + NVO concentrations exceeding those of unheated aerosol were deleted in order to be able to investigate the mixing state of the aerosol. Despite attempts to burn this possible source of organic mass off at high temperatures while sampling only particle-free air, the problem soon reappeared when sampling sea spray aerosol,

and about half of the SS + NVO measurement had to be removed from the data set.

### 3. Results and Discussion

#### 3.1. How Well Does the Sampling and Aerosol Generation Mimic Conditions at Open Sea?

[19] Natural wind generated bubble spectra have a shape similar to those shown in Figure 3, with a maximum number concentration at a diameter of about  $60\text{--}80 \mu\text{m}$  and a falloff toward larger sizes that approaches a power law,

$$dN/dr = ar^{-b}, \quad (1)$$

where  $r$  is the bubble radius [e.g., Medwin and Breitz, 1989; Bowyer, 2001; de Leeuw and Cohen, 2002; Leifer and de Leeuw, 2006].

[20] The exponent  $b$  in equation (1) is highly variable and varies with the evolution of the bubble size distribution because of the dependence of rise time on bubble size [Leifer and de Leeuw, 2006]. For instance, Bowyer [2001] found  $2 < b < 3$  near the surface and  $1 < b < 2$  near breaking waves; Medwin and Breitz [1989] found  $b = 2.7$ , while Baldy [1988] and Bezzabotnov et al. [1991] both reported  $b = 2$ . Baldy [1988] and Leifer and de Leeuw [2006] measured their spectra in a wind wave tank, the others in the real ocean; see Leifer and de Leeuw [2006] for an overview of measured bubble size distributions. As can be seen in Figure 3, the bubble spectra measured during the MAP cruise in the bubble tank peak around  $70 \mu\text{m}$ , and the exponent  $b$  is close to 2 for diameters from about  $100\text{--}1000 \mu\text{m}$  diameter,

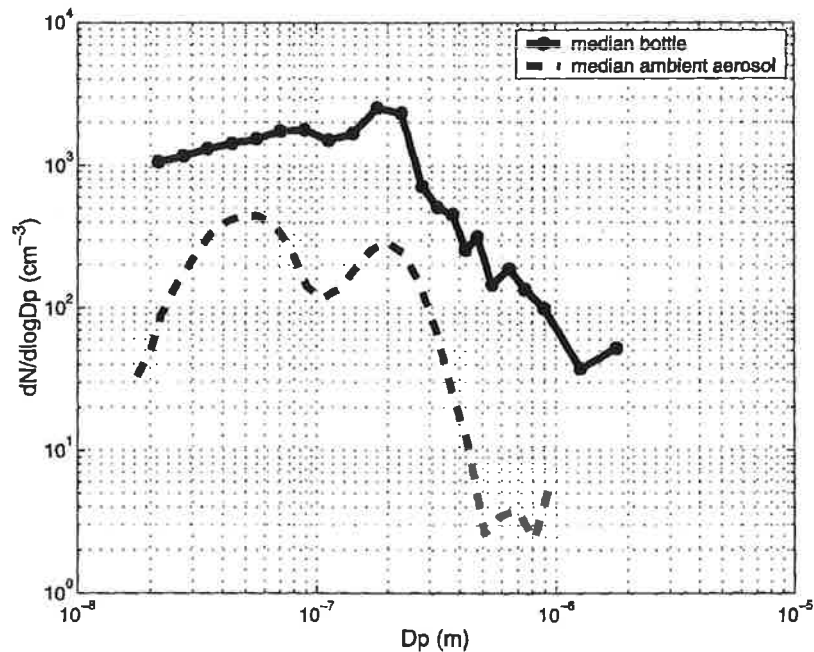


**Figure 4.** Median number size distributions produced from northeastern Atlantic water during MAP.  $D_p$  is the dry aerosol diameter. Black circles on solid line are the medians from the entire MAP campaign using the bottle ( $N = 1126$ ). Dashed curves are the medians of the clean marine ambient aerosol number size distribution during MAP ( $N = 1252$ ).

which appear to be consistent with bubble spectra near breaking waves.

[21] Figure 4 shows the ambient aerosol number size distribution sampled on the foredeck of the *Celtic Explorer* in comparison to the aerosol generated in our tank. The ambient data are representative of clean marine air with a typical marine particle concentration. We can see that the laboratory-generated aerosol size distribution is approximately a factor of 5 higher than the ambient aerosol concentration (median values of about 2000 and 400  $\text{cm}^{-3}$ , respectively). Obviously, the number size spectra of the sea spray aerosol in the tank and the ambient aerosol differ in both magnitude and shape, although the 200 nm peak is clearly visible in both spectra. *Pierce and Adams* [2006] and *Mårtensson et al.* [2007] have shown how secondary aerosol processes such as growth by condensation of secondary mass and cloud processing can modify a primary aerosol source distribution such as the one found in our tank experiment, into a typical marine aerosol size distribution sampled on the foredeck. In this process, the particles would gain more mass and size by condensation of marine sulfur compounds and probably also secondary organic compounds. Cloud processing will add additional growth above the CCN activation size, which would separate the accumulation mode from the Aitken mode as seen here in ambient data [*Hoppel et al.*, 1986]. Thus it is reasonable to assume that the produced bubble spectra, and therefore the spectral shape of the sea spray aerosol size distribution, are representative of those produced at open sea, and the aerosol in our bottle to be representative for freshly produced sea spray during the MAP cruise.

### 3.2. Aerosol Production

#### 3.2.1. Aerosol Production in the Two Tanks

[22] The average number concentration produced in the bottle was  $(2.21 \pm 1.31) \times 10^3$  particles  $\text{cm}^{-3}$  (see Table 1). To achieve better counting statistics, the system was set to produce a larger number of sea spray particles than the typical sea spray concentration found over the ocean. A concentration up to a few thousands of particles  $\text{cm}^{-3}$  is yet not enough to cause significant additional losses by coagulation considering the rapid turn-over time of the air in the bottle and sampling line. Using the bottle cross section and the sample flow, this corresponds to an average particle production of  $1.7 \times 10^6$  particles  $\text{m}^{-2} \text{s}^{-1}$ . It is of course uncertain which fraction of the bottle cross-surface area was covered with bubbles, or to what degree the walls prevented the bubbles to cover a larger surface. Yet even if it does not correspond directly to the flux from the whitecap area of a larger ocean area, this is a reasonable number for an area of high bubble and aerosol flux, comparable with *Nilsson et al.* [2001] ( $1.95 \times 10^6$  particles  $\text{m}^{-2} \text{s}^{-1}$  at  $10 \text{ m s}^{-1}$  wind speed, Arctic Ocean) and *Geever et al.* [2005] (of the order of  $2 \times 10^6$  particles  $\text{m}^{-2} \text{s}^{-1}$  at  $10 \text{ m s}^{-1}$  wind speed, northeastern Atlantic).

[23] In Figure 5, the average number and volume size distributions are shown for the whole data set with vertical bars denoting one standard deviation. To check the representativeness of the seawater sampled from the inlet at 2 m below water level, we performed a test with water collected from the surface using a bucket. The comparison of the aerosol size distributions from this experiment with those obtained with water from the ship's inlet shows that the

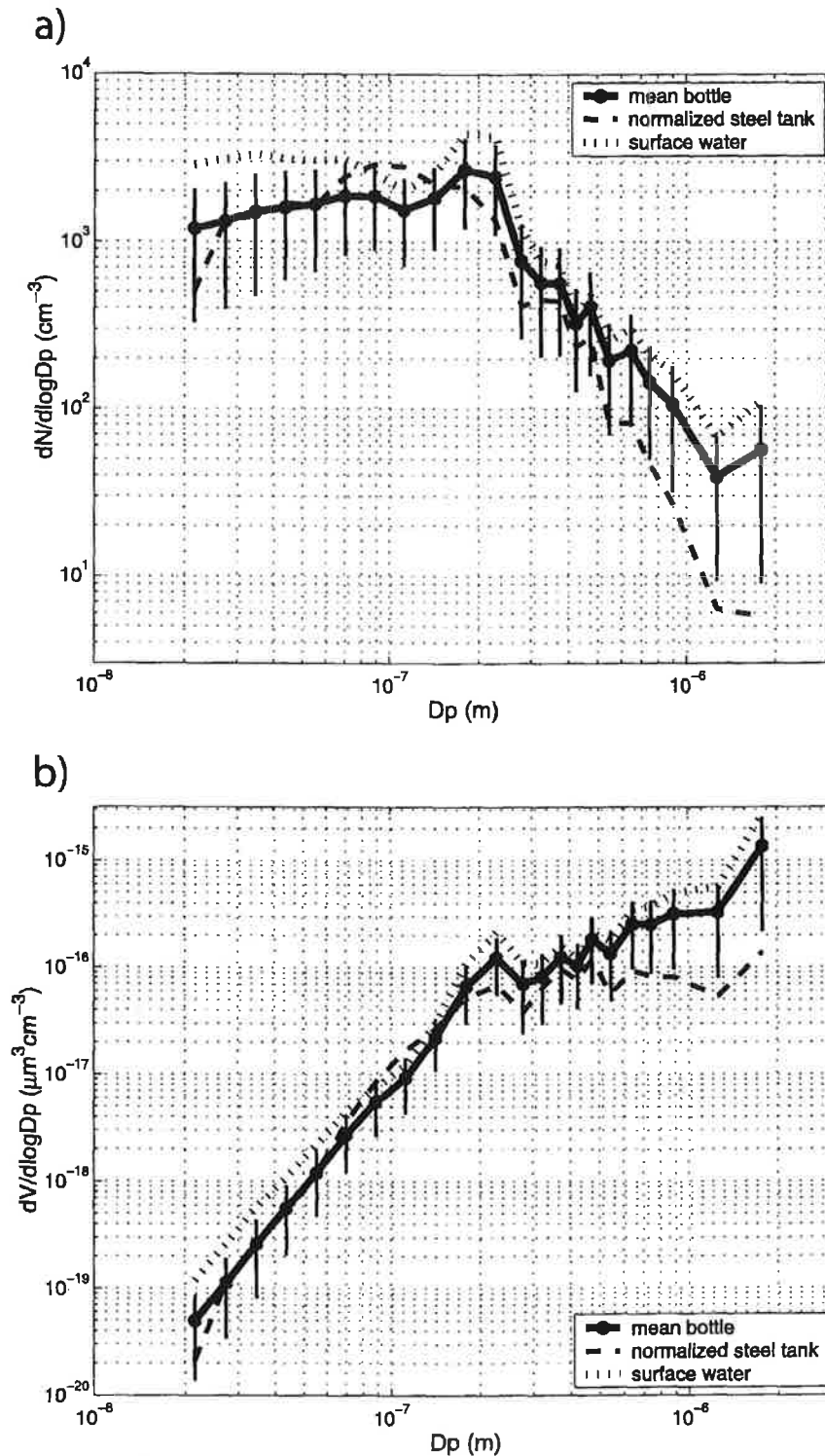


**Figure 5.** Average number and volume size distributions produced from northeastern Atlantic water during MAP.  $D_p$  is the dry aerosol diameter. (a) Black circles on solid line are the average from the entire MAP campaign using the bottle ( $N = 1126$ ). Bars denote the standard deviation centered on the mean. The dashed curve is the average of a shorter period when the same DMPS and OPC was connected to one of the steel tanks for comparison, with the concentration normalized to that of the bottle ( $N = 12$ , normalized by dividing the size distribution by the product of the total number of aerosols produced in the steel tank times the total aerosol number in the PET bottle). The dotted line shows surface water sampled with a bucket ( $N = 11$ ). (b) Same as Figure 5a, but for the volume size distribution.

**Table 2.** Overview of the Variables Considered and Their Correlation With Particle Production<sup>a</sup>

	Range, Mean and Standard Deviation	Relation to Particle Production, $r$		
		$D_p = 20-100$ nm	$D_p = 100-600$ nm	$D_p = 600-1800$ nm
<b>Water properties</b>				
Salinity (psu)	33.8–35.5, 35.4 ± 0.2	–0.27	0.04	0.18
Water temperature (°C)	12.7–16.7, 13.9 ± 0.6	–0.19	–0.44	–0.48
Dissolved oxygen (%)	89.9–107.2, 102.2 ± 2.8	–0.45	–0.65	–0.68
Chlorophyll $\alpha'$ ( $\mu\text{g L}^{-1}$ )	0.07–0.73, 0.31 ± 0.18	0.18	0.06	0.08
Dissolved organic carbon ( $\mu\text{g L}^{-1}$ )	290.9–1094.8, 691.8 ± 215.1	–0.15	–0.15	–0.18
<b>Ambient parameter</b>				
Wind speed ( $\text{m s}^{-1}$ )	0.1–16.9, 7.1 ± 4.5	0.32	0.71	0.76
<b>Tank production</b>				
Aerosol particle production ( $\text{cm}^{-3}$ )	109–7179, 2210 ± 1310	1	1	1

<sup>a</sup>The  $r$  is the Pearson's rank correlations. Number of data points:  $N_{(S, T_w, DO, \text{aerosol particle production})} = 798$ ,  $N_{(\text{Chl } \alpha')}$  = 241,  $N_{(\text{DOC})} = 18$ , and  $N_{(\text{wind speed})} = 396$ . The  $p$  is the probability that the correlation between aerosol particle production and the given parameter occurs by accident:  $p_{(S, T_w, DO, \text{aerosol particle production, Chl } \alpha', \text{ wind speed})} < 0.001$ , and  $p_{(\text{DOC})} < 0.55$ . All statistics are only for periods when the artificial sea spray size distribution was successfully sampled and may therefore differ from what is stated elsewhere for the MAP expedition.

difference in sampling methods gave at most a factor of 2.5 difference in number concentration at the smallest sizes, and the difference through most of the size range was smaller than one standard deviation (Figure 5).

[24] Also included in Figure 5 is the average distribution measured during a shorter period of sampling from the steel tank on which Berner impactors were operated for chemical sampling and analysis during most of the campaign [Facchini et al., 2008]. In Figure 5, the steel tank spectrum is normalized to the concentration in the bottle since the particle concentrations with only the DMPS + OPC sampling from the steel tank were much higher than those in the bottle. This corresponds to a higher production (on average,  $5.6 \times 10^6$  particles  $\text{m}^{-2} \text{s}^{-1}$ ), but this is, despite higher water flow of the jet, still roughly within the same order of magnitude, thanks to the larger dimensions of the steel tank. The shapes of the spectra measured in the two different containers are indeed very similar, despite the differences in jet characteristics. There is an indication of some losses of larger particles by sedimentation in the 3 m horizontal 1/4 inch steel tube that was needed to cover the distance between the aerosol instruments and the steel tank.

[25] The similar shape of the size distribution derived in the different containers, as well as the similar particle production per time and surface, suggests that the method of a vertical jet of water for bubble and sea spray production is not too sensitive to the exact shape and dimension of the tank. The actual concentration derived depends indeed on several factors (sample volume, sample flow, length of the water jet to mention some), but the aerosol size distribution is conservative, and the changes in production per surface are within the same order of magnitude. Nor does it appear to be a critical problem that the larger steel tanks were not on gimballed tables.

[26] All this supports that it is relevant to compare the physical, chemical and biological aerosol, and bubble measurements even though they were conducted in separate tanks.

### 3.2.2. Average Aerosol Size Distribution

#### 3.2.2.1. Total Aerosol Size Distribution

[27] The number production of aerosol particles peak at 200 nm  $D_p$ , but remain high at small sizes with just a weak slope, compared to the strong slope above 200 nm toward larger sizes. The aerosol volume increases sharply up to about 200 nm  $D_p$ , and above that less steeply (Figure 5).

Overall, the produced aerosol size spectra are surprisingly stable. Most of the time, the shape of the individual spectra resembles the average size spectra in its shape, although the concentrations vary. Part of the stability in size spectra can most probably be explained by the small salinity and temperature range encountered during the MAP expedition (less than 2 psu and 4°C [cf. Mårtensson et al., 2003]). Table 2 shows a summary of the considered parameters' variation and how the particle production varies with them, and Table 3 shows information about cross-correlations between all considered parameters.

[28] The current study and the recent study by Keene et al. [2007] show a mode in the vicinity of 100–200 nm with a strong slope toward the supermicrometer size (Figure 6). The similarity between the current results and Keene et al. [2007] is striking in the range above 200 nm, but they deviate below 80 nm. Although in artificial seawater, Mårtensson et al. [2003] showed a similar shape as this study, but with an overall lower concentration in the experimental bottle and with a weaker slope over the sizes. Tyree et al. [2007] on the other hand showed near lognormal modes in water from the Pacific Ocean west coast (Figure 6). Sellegri et al. [2006] interpreted the size distribution resulting from artificial salt water as a composite of three lognormal modes. The total size distribution, on the other hand, resembles the shape of the current experiment. It should be pointed out that the laboratory experiments by Keene et al. [2007] were conducted in situ, similar to our current experiment, using local water in the Sargasso Sea although the only experiment not sampling dry aerosol (instead, RH = 80%). Mårtensson et al. [2003] used only artificial salt water, while Tyree et al. [2007] used partly artificial water, and partly real seawater. But like Sellegri et al. [2006], the experiments were not conducted in situ. For example, in the case of Tyree et al. [2007], the water was sampled, transported, and stored as long as 48 h before the experiments.

[29] We can also conclude that the shape of our size distribution is in rough agreement with the field observations of sea spray emissions by Clarke et al. [2006] in the tropical Pacific Ocean. The in situ eddy covariance flux measurements by Nilsson et al. [2007] at the North Atlantic Irish coast also support a similar shape with a stronger slope above 100 nm. This implies that for  $D_p > 200$  nm, the spectral shape of the sea spray flux agrees between different

**Table 3.** Cross Correlations Between All Water Parameters and Wind Speed<sup>a</sup>

	Salinity	Water Temperature	Dissolved Oxygen	Chlorophyll $\alpha'$	Dissolved Organic Carbon	Wind Speed
Salinity	1	-0.06	-0.06	0.15	0.10	0.18
Water temperature	-0.06	1	0.55	-0.38	-0.19	-0.52
Dissolved oxygen	-0.06	0.55	1	-0.35	0.05	-0.73
Chlorophyll $\alpha'$	0.15	-0.38	-0.35	1	0.11	0.13
Dissolved organic carbon	0.10	-0.19	0.05	0.11	1	0.39
Wind speed	0.18	-0.52	-0.73	0.13	0.39	1

<sup>a</sup>The  $r$  is Pearson's rank correlations. The  $p$  is the probability that the correlation between aerosol particle production and the given parameter occurs by accident:  $p < 0.001$  for all correlations except correlations with DOC; then  $p < 0.55$ .

types of experiments at different conditions at coastal sites [Clarke *et al.*, 2006; Nilsson *et al.*, 2007] and in situ tank experiments (this study and Keene *et al.* [2007]). Although other differences in the experimental design complicate the picture, in situ sampling displays striking similarities well worth further investigating. Below 80 nm, we have an unexplained discrepancy between the various experiments, where three in situ emission measurements [Clarke *et al.*, 2006; Nilsson *et al.*, 2007; this study], and the artificial waters by Mårtensson *et al.* [2003] and Sellegri *et al.* [2006] agree on a slow slope, and as we have already observed, the other recent experiments support a near lognormal decline with decreasing size [Tyree *et al.*, 2007; Keene *et al.*, 2007]. It is hard to say if this is a real feature, as there always is a risk of losses by diffusion in the sampling systems in this size range.

### 3.2.2.2. Aerosol Size Distributions at Different Volatility

[30] From 0.02 to 0.25  $\mu\text{m}$   $D_p$ , we have also measured size distributions after heating the sea spray to 300°C. The average of this proxy for sea salt behaves in a similar manner as the unheated aerosol, as seen in Figure 7a, where also the size distribution of the aerosol burned off, interpreted as semivolatile organics, is shown. The ratio between total aerosol and SS + NVO aerosol in the 0.02–0.25  $\mu\text{m}$  interval is not constant over all sizes of particles; although in general between 5% and 33% disappear after heating (Figure 7b).

[31] According to the results of the chemical samples made in one of the larger steel tanks [Facchini *et al.*, 2008], up to 77%  $\pm$  5% of the total carbon by mass in individual submicron diameter size fractions was organic carbon. This is a seemingly much larger fraction than the difference

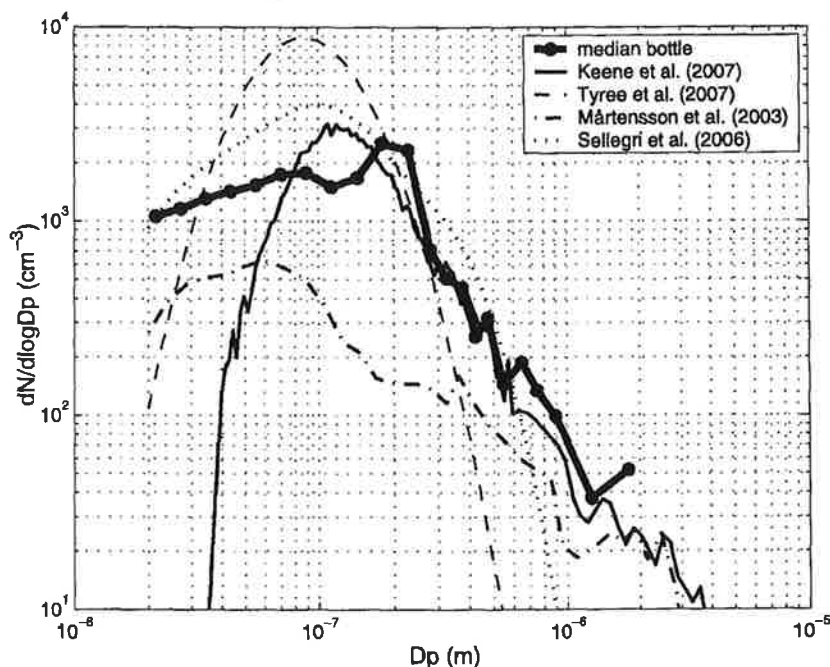


**Figure 6.** Aerosol number size distribution generated from artificial bubbles in real seawater: Median results for the MAP-06 cruise on the northeastern Atlantic (circles on bold line), example from Figure 5a of Keene *et al.* [2007] (Bermuda Institute for Ocean Sciences, 15 September 2005, thin line); a lognormal fit for the experiment FS100 in the work of Tyree *et al.* [2007] (filtered seawater from Scripps Institute of Oceanography (SIO) Pier, the dashed curve); artificial seawater from Mårtensson *et al.* [2003] (dashed/dotted line); and artificial seawater from Sellegri *et al.* [2006] (from the equation and parameters given by Sellegri *et al.* [2006, Table 1], the dotted line).

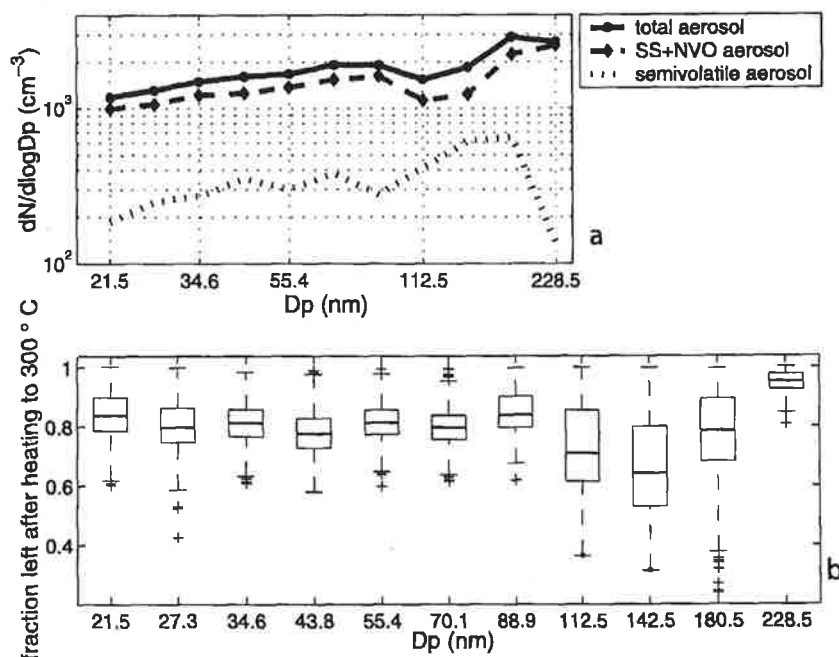


**Figure 7.** (a) Average number size distribution for the DMPS range in terms of total sea spray aerosol (circles on solid line), SS + NVO sea spray aerosol (diamonds on the dashed line), and the difference between them; semivolatile sea spray aerosol (dotted line). (b) Boxplot over the fraction left after heating to 300°C. The boxes consist of lines at the lower quartile, median, and upper quartile values. The whiskers are lines extending from each end of the box to show the extent of the rest of the data. Outliers are data with values beyond the ends of the whiskers. Number of paired data,  $N = 529$ .

between our unheated and heated observations. It is however difficult to directly compare the chemical and physical aerosol results:

[32] 1. The current estimate is number based, not mass based.

[33] 2. Sampling periods are different. As discussed later (section 3.5), we find the highest semivolatile content in the aerosol physics data within a certain wind range, which means that differences in sampling time may cause an artificial difference between physical and chemical data.

[34] 3. We have no information on whether the reduction of the aerosol concentration in a certain size channel after heating is due to loss of a number of particles of that size (externally mixed aerosol), or due to loss of part of the aerosol mass, which would lead to a size shift (internally mixed aerosol) below the detection limit of our instruments.

[35] 4. Furthermore, using 300°C to separate sea salt from organic compounds, which has become customary for marine aerosol studies as a way to separate sea-salt flux from sea spray [de Leeuw *et al.*, 2007; Nilsson *et al.*, 2007], this neglects the fact that some organic compounds known to be present in marine aerosols have higher boiling points than this. And hence incorrectly would have contributed to what we would like to define as sea salt. In retrospect, a higher temperature or scans between different temperatures might have been wiser but our choice was based both on practical arguments and on the wish to run the tank experiments so that they would be comparable with previous and parallel measurements, using 300°C.

[36] Considering statement (3), the lack of obvious size shift between the total aerosol and the SS + NVO in Figure 7a

would be consistent with an externally mixed aerosol up to about 230 nm  $D_p$ . Since a fraction of the particles evaporates completely, and a fraction of the particles leaves residuals over our detection limit of 6 nm  $D_p$ , it points directly to an external mixing of the aerosol. From eddy covariance measurements made in 2002 at Mace Head research station, west coast of Ireland, the conclusion was drawn that the measured particles over 100 nm  $D_p$  mainly consisted of internally mixed particles of semivolatile organic carbon and sea salt [Nilsson *et al.*, 2007]. The measurements were made in clean marine air during the biologically productive season, as was MAP. Considering the limited overlap in size between the data from our laboratory experiments and those from the Mace Head field experiments, this does not have to be a contradiction.

[37] One interesting question is why the bubble-bursting process would form separate sea salt and organic particles. Ellison *et al.* [1999] suggested that the organic mass fraction should approach 100% (ignoring water) below 100 nm diameter, simply for geometrical reasons: The surface film, as opposed to the bulk liquid, of each droplet would account for a larger fraction of the total volume in small particles. Some studies support the existence of purely organic sea spray particles in the size range below 200 nm [e.g., Bigg, 2007], while others show a large amount of purely sea-salt particles in this size range [Murphy *et al.*, 1998]. Our data suggest that both were produced at the same time.

[38] The bubble lifetime at the surface will change with temperature and salinity as well as by the presence of organic compounds [e.g., Thorpe, 1982; Leifer *et al.*, 2000b; Sellegri *et al.*, 2006]. Assuming that there is either

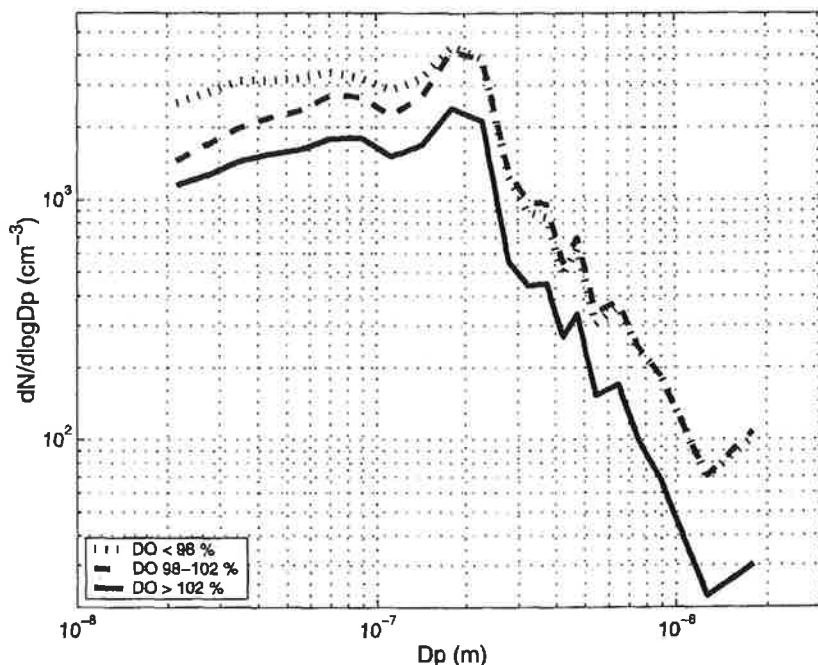


**Figure 8.** Average aerosol particle number size distributions as a function of DO, divided into subsaturated and supersaturated water (dotted and solid lines, respectively), and a near-saturated zone around 100% (dashed line). The number scans in each interval was 54 (DO < 98%), 300 (DO 98–102%), and 446 (DO > 102%).

an internal organic surface film in the bubble or on the water surface, or both, a long enough life time of the bubble will allow the bubble wall to decrease in thickness until it is entirely drained from water and consist of only the organic surfactants. At rupture, that bubble would form purely organic film drops. On the other hand, if we imagine that there are not enough surfactants to saturate the bubble surface; parts of the bubble wall may lack organic surfactants, a part which would produce pure sea-salt film drops. The surface film has been shown to break and even form a double layer if then tried to be pushed back together [Rodríguez Niño and Rodríguez Patino, 1998], and thus a yes/no regime can be anticipated in agitated environment. This would be a plausible explanation of our observations, to keep in mind for further research.

[39] The largest fraction organic material, i.e., the lowest fraction left after heating, is found in the interval 100–200 nm (see Figure 7). If this is an indication that the organic source of externally mixed particles is most pronounced in this particular size range, then it might also be part of the explanation to why there is a more distinct peak in particle production at 200 nm in this data set, in difference to other studies. *Mårtensson et al.* [2003] had a peak at 100 nm (artificial sea salt using a glass frit, salinity = 33 psu). *Keene et al.* [2007] and *Tyree et al.* [2007] also found peaks at 100 nm in laboratory experiments using a diffuser, i.e., letting air in from the bottom of the water column. This peak was present around 100 nm for different salinities, and for different concentrations of dissolved and particulate organic matter. Irrespective of the bubbling device used (weir or glass filter), *Sellegrì et al.* [2006] found a clear peak at 100 nm. However, they found that there was a

second peak at about 300–400 nm that was more pronounced when using a weir than with sintered glass filters, in better agreement with our experimental setup with a water jet (and more consistent with the natural wave breaking process).

### 3.3. Effect of Dissolved Oxygen

[40] The level of DO was here measured as percent oxygen saturation in the water, meaning the change in oxygen content since a water parcel was fully saturated at the surface (under the assumption that the water parcel remained at the surface long enough to reach full saturation) [Boyer *et al.*, 1999]. In supersaturated water, the total particle production was on average about a factor of 2 smaller than in subsaturated water (see Figure 8). Below 200 nm  $D_p$ , the trend of falling particle production continues from subsaturated, near-saturated to supersaturated water, while above 200 nm  $D_p$  the difference between near-saturated and subsaturated water is small on average. A closer look reveals that the number concentration and the DO level are best correlated for the larger particles: Above 200 nm  $D_p$ , the correlation coefficient remains better than  $r = -0.6$  (Figure 9). Below 200 nm, the correlation declines gradually for both the total aerosol number production and the SS + NVO particles, toward  $r = -0.35$ . The probability that there was no connection between the variables was in all cases  $p < 0.001$ .

[41] The saturation of ocean surface waters with respect to the major atmospheric gases (nitrogen and oxygen) can potentially affect sea spray production. When the gas pressure inside a bubble produced by a breaking wave is smaller than in the surrounding water, gas is transferred

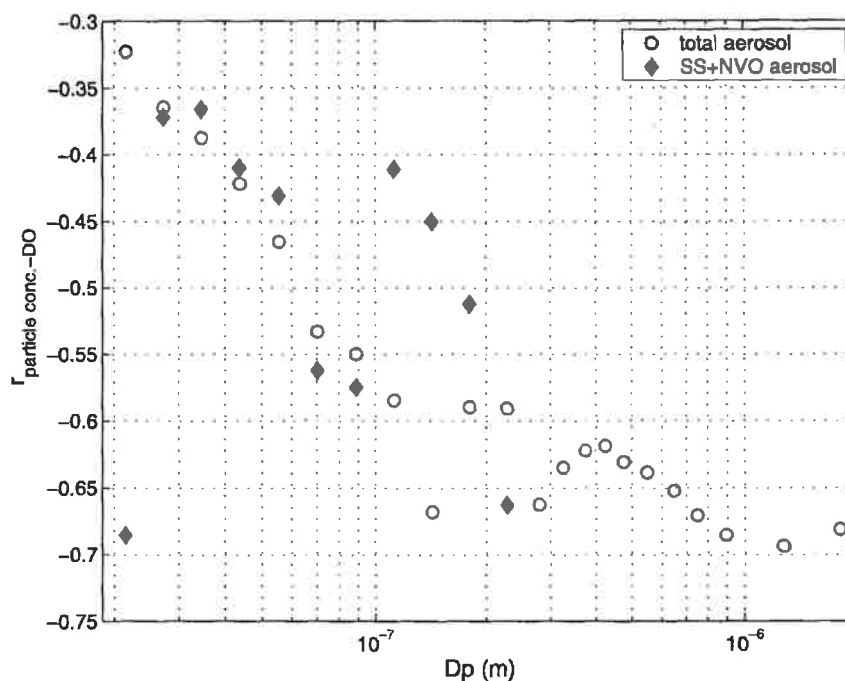


**Figure 9.** Correlation between particle production and DO for different sizes of particles (number of paired data,  $N = 800$ ). Open circles denote the total aerosol and diamonds the SS + NVO aerosol.

from ocean to the bubble, which then increases in size. The produced bubble size spectrum is clearly affected, and as a consequence, so is the resulting aerosol size spectrum [Lewis and Schwartz, 2004]. Since larger bubbles rise faster to the surface because of their buoyancy, the smallest bubbles are considered to be most affected by this process. As the aerosol measured in the current size range is expected to result from film drops, parented by rather large bubbles (above  $D_b = 2$  mm), they should theoretically not be much affected.

[42] The effect on aerosol production from variations in DO was illustrated by Stramska *et al.* [1990]. These authors found that more aerosol droplets (diameter  $> 0.5 \mu\text{m}$ ) were produced in supersaturated water than in subsaturated water and derived the following relation between droplet production and salinity:  $N(D > 0.5 \mu\text{m}) = 5.54 \times 10^5 e^{0.0291s}$ , where  $s$  is the percentage of oxygen saturation. Unfortunately, it is not clear whether the variation observed by Stramska *et al.* [1990] was in full related to oxygen levels, as the different oxygen saturations were reached by varying the water temperature.

[43] Dissolved oxygen is governed by changes in the biological activity of the water column as well as by physical factors such as advection of ocean waters, or exchange due to turbulent and diffusive transport across the ocean surface skin layer caused by wind speed and bubbles [e.g., Craig and Hayward, 1987, McNeil *et al.*, 1995, Boyer *et al.*, 1999; Frew *et al.*, 2004]. This dual influence and the relative contribution of each factor have been debated [Craig and Hayward, 1987] and may vary from one water body to another and with season. Our experiments did not reveal a diurnal variation between DO and particle production, possibly because of the variability of the algae bloom as the ship moved through

different areas. As for the physical contribution, the maximum DO concentration in water is also a function of both temperature and salinity; more oxygen can be solved in less saline water and at lower temperatures [Wanninkhof, 1992; Boyer *et al.*, 1999], where the effect of salinity is small compared to the effect of water temperature. The small range in salinity and water temperature during MAP (again, less than 2 psu and  $4^\circ\text{C}$ ) limits our ability to investigate the influences of these parameters thoroughly. Despite this, we detect a significant correlation between DO and water temperature ( $r = 0.55$ ,  $p < 0.001$ ; see Table 3), although the relationship reflects an increase of DO with water temperature instead of the above mentioned expected decrease. The conclusion is that the temperature effect on DO is outranked here, possibly by biological activity, since higher biological photosynthetic activity is bound to increase during hours of daylight (and higher temperatures). Although the actual contribution to a change in total gas saturation due to biological activity is considered to be approximately a factor of 3 lower than the actual change in oxygen saturation (for example: A DO saturation of 115%, results in a total gas anomaly of only 5%) [Lewis and Schwartz, 2004], making the physical effects of DO saturation as influenced by biology not a key suspect as responsible of the decreased particle production. However, biological activity can possibly alter the surface-active material present and/or the surface tension and therefore take the particle production in the opposite direction than expected from the, by physical properties, increased DO alone.

### 3.4. Effect of Chlorophyll

[44] We attempted to use chlorophyll  $\alpha'$  as a marker for biological activity, with the assumption that high

chlorophyll  $\alpha'$  would indicate recent growth and thus accumulation of chlorophyll-containing microorganisms, primarily algae. However, Table 2 shows that the correlation between aerosol number and chlorophyll at best is  $r = -0.18$  ( $p < 0.001$ ), this corresponding to the production of particles of  $D_p = 600\text{--}1800$  nm. Both water temperature and DO in the water decreases slightly with increasing chlorophyll  $\alpha'$  (the correlation coefficients are  $-0.38$  and  $-0.35$ , respectively,  $p < 0.001$ ; see Table 3), and it should be clarified that the maximum concentration of chlorophyll in ocean water does not have to coincide with the peak of photosynthesis (and oxygen production) on a short time scale (early examples are found in the work of Lorenzen [1963] and Marra [1978]).

[45] Organic material in the water plays a critical role in marine chemistry and may do so for the aerosol composition as well, and photosynthetic marine organisms are one source of organic material (others may be river run off, atmospheric deposition and decomposition of dead marine organisms). One of our working hypotheses within the MAP project was that there could be a relationship we could parameterize from our observations and use in satellite data analysis (where chlorophyll  $\alpha$  proxies are available) and models as a way of estimating the biological influence on the particle production and composition. There is no question to whether organic marine substances are, or can be, part of the marine aerosol. O'Dowd *et al.* [2004, 2008] found a correlation between chlorophyll and organic aerosol mass at the Irish west coast. During summer, in times of high chlorophyll concentrations, they found the maximum production. Perhaps a close relationship between chlorophyll concentrations and particle production could not be expected during MAP. For example, an important parameter overlooked comparing these data is the time frame in which the photosynthesis is able to cause enough of the particular organics we encounter in our aerosol, and the time resolution in which we will be able to observe this. We can make an analogy with the production and emission of dimethylsulfide (DMS). Although the release of DMS originates from biological production, it is not released until a series of complex chemical reactions, acting either as sinks or sources, and grazing has occurred. The result is a complex relationship between chlorophyll and DMS [Gröne, 1995]. Although we know little about the system we have begun to study, the organic surfactants we are interested in are not among the hydrocarbons (sugars) produced directly by photosynthesis. On the long time scale and large space scale where organic aerosol mass (weeklong sampling time) and chlorophyll (spatial scale of the satellite data) correlate with the work of O'Dowd *et al.* [2008], primary production by photosynthesis may have reached all the way into the organic aerosol mass. On the local and short 10 min time scale we work in the current study, it is not surprising that such a relationship is absent. In high-productive waters, surfactant organics may be present in excess of what can be efficiently injected into the atmosphere by physical processes [e.g., Tyree *et al.*, 2007]. But even though this cruise took place in high-productive waters, at times of successful bubble-bursting measurements the level of chlorophyll  $\alpha'$  was below the highest chlorophyll level reported in the work of O'Dowd *et al.* [2008], at most  $0.75 \mu\text{g L}^{-1}$ . Nonetheless, we have to

conclude that in our data set there is no relationship between chlorophyll  $\alpha'$  and sea spray production, either because there is no biological influence on the sea spray production, or that this is more complex and perhaps dependent on more specific compounds or other species than the chlorophyll  $\alpha$  proxy. For instance, some algae produce lipids for buoyancy, and therefore add to the surfactant pool only once they break, i.e., when the bloom comes to an end when nutrients have been exhausted. Thus the dynamics of the microorganism community will affect the abundance of rich film occurrence.

[46] Real seawater implies a considerable fraction of organic carbon in the water. Most organic surface active material lowers the surface tension of water, and therefore bubbles are not as easily produced on the water surface [Thorpe, 1982; Blanchard, 1983]. Already Blanchard [1963] and Paterson and Spillane [1969] showed that the production of film drops was significantly reduced by the presence of surfactants. A high concentration of organic surface-active material was later observed to diminish production of both jet and film drops from the water surface [Weber *et al.*, 1983]. Note that it is entirely possible that an increased content of organic surfactants could decrease the number production of particles while those particles that are produced contain more organic mass. Leifer *et al.* [2000b] observed that the velocity with which the bubbles rise to the surface decreased when they became contaminated with surfactants, which also could reduce the production of aerosol particles. In summary, while the results of O'Dowd *et al.* [2004, 2008] and Facchini *et al.* [2008] suggest that marine organic matter through sea spray contributes to a large fraction of organic matter in marine aerosol mass, it may in fact reduce the produced aerosol number. Furthermore, the absence of a correlation with chlorophyll  $\alpha'$  suggests that the particle production is not directly linked to photosynthesis and its primary hydrocarbon products, rather may require additional biological and chemical process steps.

### 3.5. Effect of Ambient Wind Speed

[47] While it is well known that real ocean sea spray production is strongly dependent on wind speed, there is of course no wind inside the tank where the measurements were made. So why compare the data with the ambient wind? The wind speed is such a dominant parameter that in ambient measurements, it often obscures the effects of other parameters, which is one of the reasons for making this experiment at all. Furthermore, if there are secondary effects of wind speed other than the obvious and immediate effect of more breaking waves as a result of higher wind speed, these could possibly be revealed by the laboratory aerosol data. In Figure 10, one can see that, in general, more particles on average are produced at higher wind speed. The effect is most pronounced in the number of semivolatile particles in the 100–250 nm size range, where most CCN would be expected to be found. The production is approximately doubled below 100 nm and tripled between 100 and 250 nm (see Figure 11). The largest number of events occurred at low to moderate wind speeds (seven each), while at the 10–15  $\text{m s}^{-1}$  wind speeds there were only three events, and at higher wind speeds there were two measurements.

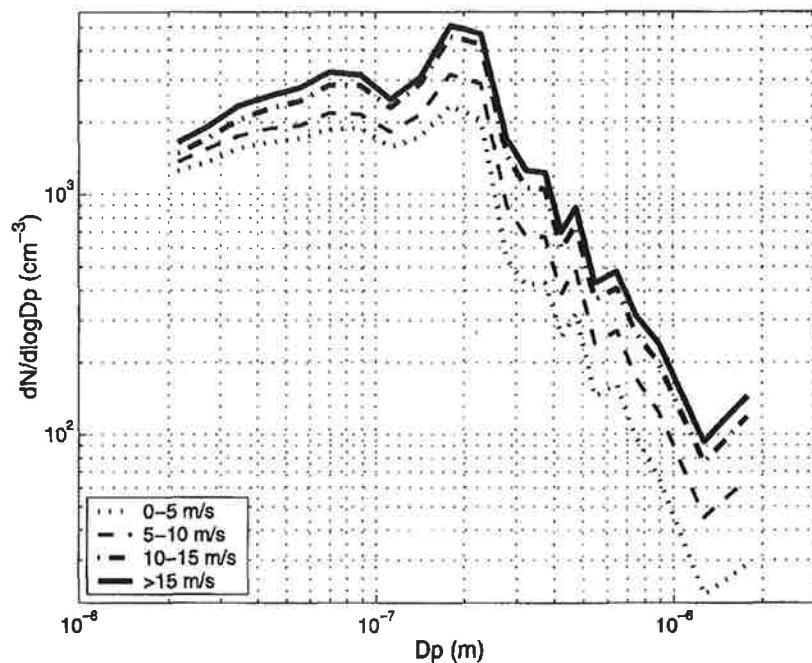


**Figure 10.** Average aerosol size distributions produced in the tank at different wind speeds. The number of scans in each interval is 179 ( $0-5 \text{ m s}^{-1}$ , dotted line), 112 ( $5-10 \text{ m s}^{-1}$ , dashed line), 87 ( $10-15 \text{ m s}^{-1}$ , dash-dotted line), and 19 ( $>15 \text{ m s}^{-1}$ , solid line).

[48] The result is somewhat puzzling, considering that we are not looking at ambient particle concentrations or production, where an increase with the wind speed would be natural [Nilsson *et al.*, 2001, 2007], but looking at data from within a tank where there is no wind. A possible

explanation would be that the inlet used for sampling was not close enough to the surface to sample organic surfactants at low wind speed when much of these could be confined to a surface film. Some factors speak against this.

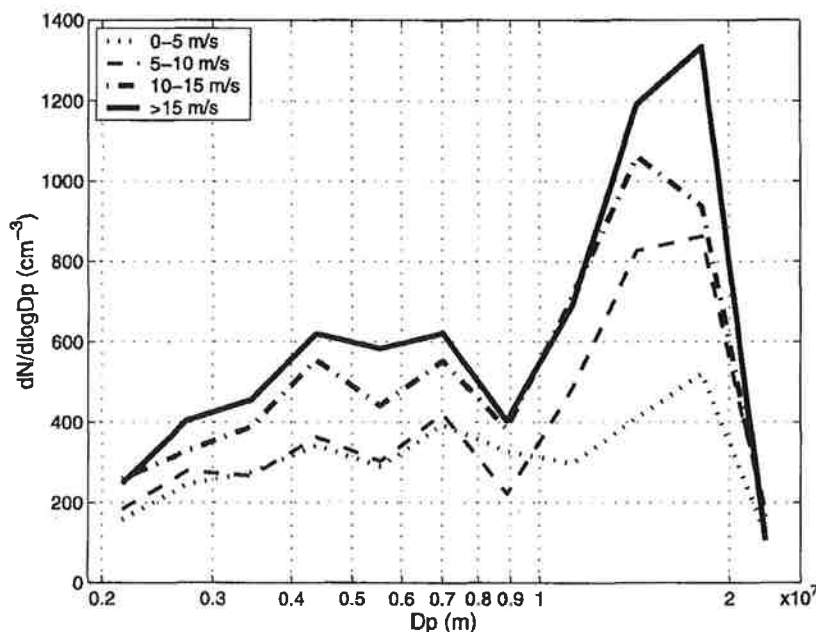


**Figure 11.** Average semivolatile aerosol at different wind speeds, denoted in the same way as in Figure 10. The number of scans in each interval is 96 ( $0-5 \text{ m s}^{-1}$ ), 51 ( $5-10 \text{ m s}^{-1}$ ), 47 ( $10-15 \text{ m s}^{-1}$ ), and 9 ( $>15 \text{ m s}^{-1}$ ).

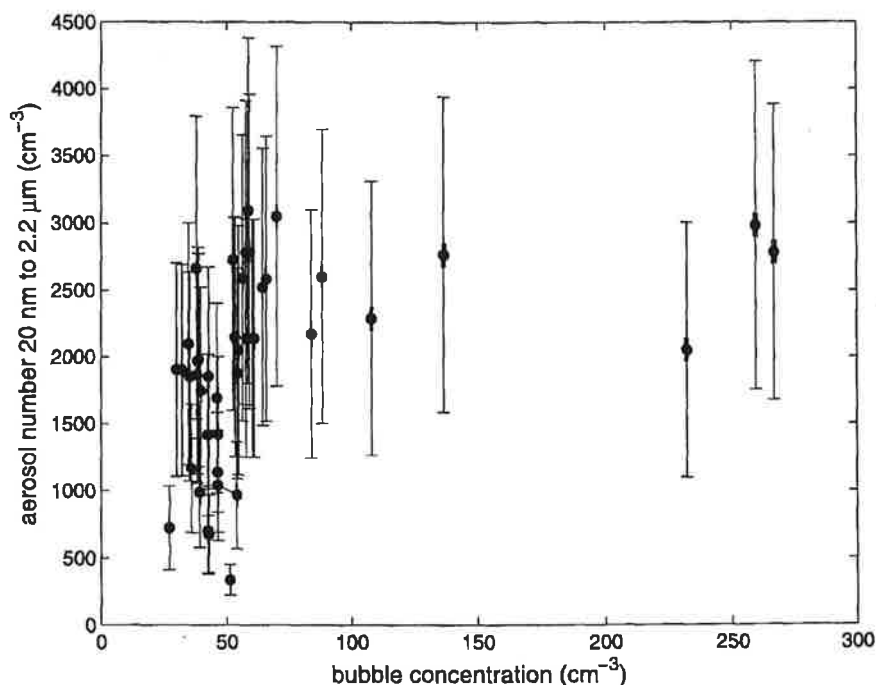


**Figure 12.** Aerosol number concentration in the bottle compared to the bubble number concentration. Error bars denote one standard deviation. Number of paired data,  $N = 43$ .

[49] 1. There was still plenty of organic matter in the aerosol produced in the larger steel tank from the same sampling line, and the majority of this was water insoluble [Facchini *et al.*, 2008].

[50] 2. The test sampling directly from the surface resulted in an aerosol production that is close to the aerosol production in water sampled through the  $-2$  m inlet (Figure 5). Where it deviates, the surface water, which if this was a problem should contain more organic matter, deviates positively from the inlet water (more particles), in contrast to previous research on the effects of surfactants on aerosol production.

[51] 3. Since no breaking waves at all form below about  $4 \text{ m s}^{-1}$  [Monahan and O'Muircheartaigh, 1980], unbroken surface films should have been most predominant during those conditions, and we would have expected more of a stepwise change between the first two wind intervals. Instead, we find only a continuous increase in Figures 10 and 11. In Figure 11, the semivolatile aerosol does not change at all from  $0$ – $5$  to  $5$ – $10 \text{ m s}^{-1}$  below  $100 \text{ nm}$  dry diameter.

[52] 4. In addition, although the use of the  $-2$  m sampling line was a practical necessity, one has to consider that  $2 \text{ m}$  is an average depth. In all but a very calm sea, the actual sampling depth will vary around this level, and the actual water flow will include a fraction that is sampled even closer to the surface. While sampling directly at the surface would be preferable it is probably not a critical problem.

[53] But what did then cause this trend with wind speed? In Table 3, one can see strong negative relationships between wind speed and both DO and water temperature ( $r = -0.73$  and  $r = -0.52$  respectively,  $p < 0.001$ ), as well as a weak indication of an increase of DOC ( $r = 0.39$ , although with a low statistical significance;  $p < 0.55$ ). Wind

speed causes advection of surface water as well as upward mixing of deeper water, which can possibly be both colder, more oxygen deficient, and chemically different, contributing to a change in both aerosol production and the actual aerosol composition.

### 3.6. Bubble Spectra

[54] In Figure 12, we compare aerosol number concentrations in the head space of the bottle to simultaneously measured bubble number concentrations in the open steel tank. The aerosol number concentration increases rapidly with bubble concentration up to a maximum of about  $3000 \text{ particles cm}^{-3}$  produced from about  $60 \text{ bubbles cm}^{-3}$ . For larger bubble concentrations, the number of particles seems to plateau at a value between  $2500$ – and  $3000 \text{ particles cm}^{-3}$ . In terms of aerosol production per bubble, this corresponds to a steep increase toward  $40$ – $50 \text{ particles per bubble}$  near  $50$ – $60 \text{ bubbles cm}^{-3}$  and thereafter a gradual decrease which approaches  $10 \text{ particles per bubble}$ . Throughout, all sizes the aerosol is positively correlated with bubbles smaller than about  $200$ – $250 \mu\text{m}$ .

[55] There are unfortunately too few observations to substantiate this behavior, nor do we have an explanation for it. A more detailed comparison size bin by size bin shows that the best correlations are found between bubbles of  $D_b < 50 \mu\text{m}$  and particles of  $D_p < 40 \text{ nm}$  ( $r = 0.4$ ,  $p < 0.001$ ), and between  $D_b = 300$ – $500 \mu\text{m}$  and  $D_p = 600 \text{ nm}$  to  $1.8 \mu\text{m}$  ( $r = -0.4$ ,  $p < 0.001$ ); Figure 13.

[56] Apart from the weak correlation mentioned in the previous paragraph, the long slope in the bubble spectra from  $250 \mu\text{m}$  to  $1 \text{ mm}$  ( $dN/dr = 270 r^{-2}$ ; see Figure 3) is hardly correlated with particle production. Following previous studies, the produced particles should dominantly come from film drops, and these should primarily be formed

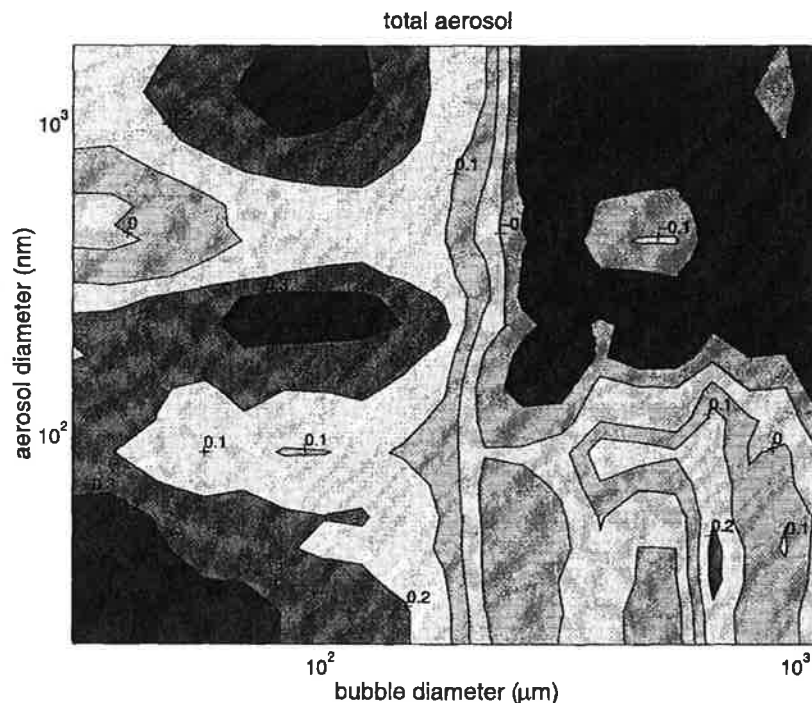


**Figure 13.** Size resolved correlations between the bubble concentration ( $x$  axis) and total aerosol concentration ( $y$  axis). Number of paired data,  $N = 79$ , and  $p < 0.001$ .

from bubbles that are larger than 2–2.5 mm [Blanchard and Syzdek, 1988; Resch and Afeti, 1992], a bubble size exceeding our detection limit. Observations show that equation (1) well describes the oceanic background spectra [Leifer and de Leeuw, 2006]. However, the larger bubbles produced immediately after wave breaking rise rapidly to the surface under the influence of their buoyancy, and hence the question arises of how representative our observations could be for these larger bubbles since we measure the bubbles below the surface (given they would be included in our detection limit). For instance, observations by Leifer and de Leeuw [2006] show the time evolution of bubble plumes in a fresh water tank with a fast change of the exponent  $b$  in consequence of the loss of larger bubbles. For open sea, bubble spectra have been observed that confirm that the larger bubbles are more populous nearer to the surface [Medwin and Breitz, 1989]. Hence their concentrations may be large enough to produce significant amounts of film droplets. A similar situation may have occurred in our jet experiments, but we have no material, nor the instrumentation, to check the full bubble profile.

[57] The next important question that arises from Figure 12 is, What are the possible reasons for the observed behavior of the number of particles versus the bubble concentrations? In other words, why does the number of particles formed per bubble first increase toward 40–50 particles per bubble and then decreases and levels off at about 10 particles per bubble? Both are well above the maximum number of jet drops that is supposed to form per bubble [Cipriano and Blanchard, 1981], but below the maximum number of film droplets formed from a bubble with a diameter of several millimeters [Blanchard and Syzdek, 1988; Resch and Afeti, 1992]. In the first case, it

appears that our data support an additional or even alternative source of a large number of particles besides the traditional film drops shown to result from giant bubbles. A possibility to consider is the existence of secondary bubbles that has been observed to form right after the rupture of larger bubbles [Leifer et al., 2000a], that may even have jet drops in the submicrometer size range, and that is below the lower size cut of our bubble sizer and of most other such instruments. In the later case, we can so far only speculate that Figure 12 reveals an effective maximum of particles that can effectively form from bubbles in highly biologically active salt water.

#### 4. Summary and Conclusions

[58] The current experiment was designed to study the primary marine aerosol production from breaking waves during a cruise that was part of the MAP project. The investigation was made on board the *Celtic Explorer* on the northeastern Atlantic. Water was continuously sampled from an average depth of 2 m below the water surface to produce a jet of water to simulate the action of breaking waves in several tanks and the ensuing production of bubbles and aerosol droplets. The physics of the produced aerosol and its chemical and biological content were characterized, together with bubble spectra and water chemistry, all conducted in parallel in the ship laboratory. Here the focus has been on the aerosol physics, and its dependence on other parameters. The main conclusions are as follows.

[59] 1. The bubble spectra produced in the laboratory tank using a jet of water impinging on a water surface was realistic and representative of near surface spectra in the vicinity of breaking waves. As the aerosol spectra are

direct results of the produced bubble spectra, we therefore expect the aerosol spectra to be realistic as well.

[60] 2. The produced aerosol number spectra peaked at about  $D_p = 200$  nm with a strong decrease of the concentrations toward larger sizes and a weaker decrease toward smaller sizes, and the spectral shape was conservative throughout the cruise. A comparison with previous experiments is complicated because of methodological differences, although reveals large similarities of the spectral shape over  $D_p > 200$  nm for in situ experiments, while tank experiments using transported and stored water deviated more. Over  $D_p = 200$  nm, there is also an agreement between the current experiment and field observations of sea spray emissions, further supporting the benefits of in situ sampling.

[61] 3. The largest fraction of semivolatile organic aerosol is found around 100–200 nm  $D_p$  and below 230 nm the produced aerosol seems to be externally mixed. Previous research has shown various results on the subject, and the contribution to the question by the current study is speculated to occur when the rising bubbles are not saturated with organic material, causing both pure organic aerosol and sea-salt aerosol to be produced simultaneously.

[62] 4. The level of DO comes out as the water parameter best correlated with the aerosol production, where the correlation for  $D_p > 200$  nm remains stronger than  $r = -0.6$  ( $p < 0.001$ ). A change in saturation of DO in surface water can possibly affect the sea spray production because of its influence on the bubble size distribution. The DO range observed is though considered to be too narrow to have a major effect on the bubble size distribution, especially for the large ( $D_b > 2$  mm) bubbles previously shown to be required to produce aerosol in our size range. Instead, as the changes in DO are argued to be a product of biological activity, the possibility of an altered surface chemistry accompanied by increased surfactant concentration as a result of biology is thought to diminish the particle production.

[63] 5. The aerosol number production, under these circumstances, is not influenced by the ocean chlorophyll level, indicating that the hydrocarbons produced directly by the photosynthesis are not essential for the sea spray production on this short time scale. We speculate that such a correlation perhaps could be found using a longer time frame. The chemistry associated with an algae bloom is complex, and needs to be well monitored in order to explore a relationship like this.

[64] 6. The ambient wind speed appears to have a secondary effect on the particle production other than the influence on the amount of whitecaps, as both the total and the semivolatile organic fraction of the sea spray number production in our laboratory tank increases with the ambient wind speed. The enhanced upward mixing of possibly chemically different water of lower temperature and oxygen saturation to the ocean surface at high wind speed strongly affects the aerosol particle production, and should be taken into account when investigating the production and composition of sea spray at high wind speed.

[65] 7. In our size ranges, about 30–1000  $\mu\text{m}$   $D_b$  and 0.020–1.8  $\mu\text{m}$   $D_p$ , the best correlation between bubbles and aerosol particles are between bubbles of  $D_b < 50$   $\mu\text{m}$  and particles of  $D_p < 40$  nm ( $r = 0.4$ ,  $p < 0.001$ ) and between  $D_b = 300$ –500  $\mu\text{m}$  and  $D_p = 600$  nm–1.8  $\mu\text{m}$  ( $r = -0.4$ ,

$p < 0.001$ ). The maximum particle production per bubble under these circumstances is about 40–50 bubbles per  $\text{cm}^3$ . To understand this behavior, further research is needed which should include larger bubble sizes (over  $D_b = 2$  mm), more inclined to produce the aerosol in the submicrometer size range.

[66] The benefit of studying sea spray production during a laboratory experiment on a ship at the open ocean includes the possibility of finding biologically highly productive water to investigate a relationship between aerosol production and chlorophyll in real seawater unperturbed by transport and storage from the sea to a laboratory ashore. To be able to study this relationship, it is now clear that longer sampling periods are needed. Preferably, sampling should take place on a fixed location to study effects of diurnal variation in temperature and DO. More detailed water chemistry, higher time resolution of the aerosol chemical sampling, a wider size range of bubble measurements (to include the very large millimeter sized bubbles), and surface tension measurements would further improve the possibilities of successfully explaining and parameterizing the sea spray production.

[67] **Acknowledgments.** The MAP (Marine Aerosol Production from natural sources) project is financially supported by the European Commission (FP6, project number 018332) and participating institutes. Further financial support was received from Swedish Research Council (VR), and the Swedish Research Council on Environment Agricultural Science and Spatial Planning (FORMAS). Special thanks are due to Lars Ahlm, Paul Glanz, Leif Bäcklin, Dag Broman, Juri Wahler, and Kai Rosman during the preparations, construction work, installations, repair, and demobilization before and after the cruise. We are most obliged to the Marine Institute for their assistance before and during the cruise and to the crew of the *Celtic Explorer*. We would like to thank Bill Keene for providing us with data for Figure 13 from Keene *et al.* [2007], Janina Woeltjen at University of East Anglia for the chlorophyll  $\alpha$  calibration, and Leo Cohen of TNO D&V for the bubble measurements.

## References

- Afeti, G. M., and F. J. Resch (1990), Distribution of the liquid aerosol produced from bursting bubbles in sea and distilled water, *Tellus, Ser. B*, 42, 378–384.
- Andreas, E. L. (1998), A new sea spray generation function for wind speeds up to  $32 \text{ m s}^{-1}$ , *J. Phys. Oceanogr.*, 28, 2175–2184.
- Baldy, S. (1988), Bubbles in the close vicinity of breaking waves: Statistical characteristics of the generation and dispersion mechanism, *J. Geophys. Res.*, 93(C7), 8239–8248.
- Baron, P. A., and K. Willeke (2005), *Aerosol Measurements: Principles, Techniques, and Applications*, 2nd ed., Wiley-Intersci., New York.
- Bezzabotnov, V. S., A. K. Degterev, and V. N. Emereev (1991), Determination of gas exchange rate in whitecaps using measurements of the bubble concentration, *Sov. J. Phys. Oceanogr.*, 2(3), 221–225.
- Bigg, E. K. (2007), Sources, nature and influence on climate of marine airborne particles, *Environ. Chem.*, 4, 155–161, doi:10.1071/EN07001.
- Blanchard, D. C. (1963), The electrification of the atmosphere by particles from bubbles in the sea, *Prog. Oceanogr.*, 1, 73–202.
- Blanchard, D. C. (1983), The production, distribution, and bacterial enrichment of the sea-salt aerosol, in *Air-Sea Exchange of Gases and Particles*, edited by P. S. Liss and W. G. N. Slinn, pp. 407–454, Reidel, Dordrecht, Netherlands.
- Blanchard, D. C., and L. D. Syzdek (1982), Water-to-Air transfer and enrichment of bacteria in drops from bursting bubbles, *Appl. Environ. Microbiol.*, 43(5), 1001–1005.
- Blanchard, D. C., and L. D. Syzdek (1988), Film drop production as a function of bubble size, *J. Geophys. Res.*, 93(C4), 3649–3654.
- Bowyer, P. A. (2001), Video measurements of near-surface bubble spectra, *J. Geophys. Res.*, 106(C7), 14,179–14,190.
- Boyer, T., M. E. Conkright, and S. Levitus (1999), Seasonal variability of dissolved oxygen, percent oxygen saturation, and apparent oxygen utilization in the Atlantic and Pacific Oceans, *Deep Sea Res., Part 1*, 46, 1593–1613.

- Brooks, B. J., M. H. Smith, M. K. Hill, and C. D. O'Dowd (2002), Size-differentiated volatility analysis of internally mixed laboratory-generated aerosol, *J. Aerosol Sci.*, **33**, 555–579.
- Cavalli, F., et al. (2004), Advances in characterization of size-resolved organic matter in marine aerosol over the North Atlantic, *J. Geophys. Res.*, **109**, D24215, doi:10.1029/2004JD005137.
- Charlson, R. J., S. E. Schwartz, J. M. Hales, R. D. Cess, J. A. Coakley Jr., J. E. Hansen, and D. J. Hofmann (1992), Climate forcing by anthropogenic aerosols, *Science*, **255**, 423–430.
- Cipriano, R. J., and D. C. Blanchard (1981), Bubble and aerosol spectra produced by a laboratory breaking wave, *J. Geophys. Res.*, **86**(C9), 8085–8092.
- Cipriano, R. J., D. C. Blanchard, A. W. Hogan, and G. G. Lala (1983), On the production of Aitken nuclei from breaking waves and their role in the atmosphere, *Am. Meteorol. Soc.*, **40**(2), 469–479.
- Clarke, A. D., S. R. Owens, and J. Zhou (2006), An ultrafine sea-salt flux from breaking waves: Implications for cloud condensation nuclei in the remote marine atmosphere, *J. Geophys. Res.*, **111**, D06202, doi:10.1029/2005JD006565.
- Craig, H., and T. Hayward (1987), Oxygen supersaturation in the ocean: Biological versus physical contributions, *Science*, **235**, 199–202.
- de Leeuw, G., and L. H. Cohen (2002), Bubble size distributions on the North Atlantic and North Sea, in *Gas Transfer and Water Surfaces*, *Geophys. Monogr. Ser.*, vol. 127, edited by M. A. Donelan et al., pp. 271–277, AGU, Washington, D. C.
- de Leeuw, G., M. Moerman, C. J. Zappa, W. R. McGillis, S. Norris, and M. Smith (2007), Eddy correlation measurements of sea spray aerosol fluxes, in *Transport at the Air Sea Interface*, edited by C. S. Garbe, R. A. Handler, and B. Jähne, pp. 297–311, Springer, Berlin.
- Ellison, G. B., A. F. Tuck, and V. Vaida (1999), Atmospheric processing of organic aerosols, *J. Geophys. Res.*, **104**(D9), 11,633–11,641.
- Facchini, M. C., et al. (2008), Primary submicron marine aerosol dominated by insoluble organic colloids and aggregates, *Geophys. Res. Lett.*, **35**, L17814, doi:10.1029/2008GL034210.
- Frew, N. M., et al. (2004), Air-sea transfer: Its dependence on wind stress, small-scale roughness, and surface films, *J. Geophys. Res.*, **109**, C08S17, doi:10.1029/2003JC002131.
- Geever, M., C. D. O'Dowd, S. van Ekeren, R. Flanagan, E. D. Nilsson, G. de Leeuw, and U. Rannik (2005), Submicron sea spray fluxes, *Geophys. Res. Lett.*, **32**(15), L15810, doi:10.1029/2005GL023081.
- Gong, S. L. (2003), A parameterization of sea-salt aerosol source function for sub- and super-micron particles, *Global Biogeochem. Cycles*, **17**(4), 1097, doi:10.1029/2003GB002079.
- Gong, S. L., L. A. Barrie, and J.-P. Blanchet (1997a), Modeling sea-salt aerosols in the atmosphere: 1. Model development, *J. Geophys. Res.*, **102**(D3), 3805–3818.
- Gong, S. L., L. A. Barrie, J. M. Prospero, D. L. Savoie, G. P. Ayers, J.-P. Blanchet, and L. Spacek (1997b), Modeling sea-salt aerosols in the atmosphere: 2. Atmospheric concentrations and fluxes, *J. Geophys. Res.*, **102**(D3), 3819–3830.
- Gröne, T. (1995), Biogenic production and consumption of dimethylsulfide (DMS) and dimethylsulfoniopropionate (DMSP) in the marine epipelagic zone: A review, *J. Mar. Syst.*, **6**, 191–209.
- Hinds, W. C. (1999), *Aerosol Technology: Properties, Behavior and Measurements of Airborne Particles*, 2nd ed., Wiley-Intersci., New York.
- Hoppel, W. A., G. M. Frick, and R. E. Larson (1986), Effect of nonprecipitating clouds on the aerosol size distribution in the marine boundary layer, *Geophys. Res. Lett.*, **13**(2), 125–128.
- Intergovernmental Panel on Climate Change (IPCC) (2007), *Climate Change 2007: The Physical Science Basis—Contribution of Working Group I to the Fourth Assessment Report of the Intergovernmental Panel on Climate Change*, 996 pp., edited by S. Solomon et al., Cambridge Univ. Press, Cambridge, U. K.
- Jarvis, N. L., W. D. Garrett, M. A. Scheimann, and C. O. Timmons (1967), Surface chemical characterization of surface-active material in seawater, *Limnol. Oceanogr.*, **12**(1), 88–96.
- Jokinen, V., and J. M. Mäkelä (1997), Closed-loop arrangement with critical orifice for DMA sheath/excess flow system, *J. Aerosol Sci.*, **28**(4), 643–648.
- Keene, W. C., et al. (2007), Chemical and physical characteristics of nascent aerosols produced by bursting bubbles at a model air-sea interface, *J. Geophys. Res.*, **112**, D21202, doi:10.1029/2007JD008464.
- Kuznetsova, M., C. Lee, and J. Aller (2005), Characterization of the proteinaceous matter in marine aerosols, *Mar. Chem.*, **96**, 359–377.
- Lamarre, E., and W. K. Melville (1992), Instrumentation for the measurement of void-fraction in breaking waves: Laboratory and field results, *IEEE J. Oceanic Eng.*, **17**(2), 204–215.
- Leifer, I., and G. de Leeuw (2006), Bubbles generated from wind-steepened breaking waves: I. Bubble plume bubbles, *J. Geophys. Res.*, **111**, C06202, doi:10.1029/2004JC002673.
- Leifer, I., G. de Leeuw, and L. H. Cohen (2000a), Secondary bubble production from breaking waves: The bubble burst mechanism, *Geophys. Res. Lett.*, **27**(24), 4077–4080.
- Leifer, I., R. K. Patro, and P. Bowyer (2000b), A study on the temperature variation of rise velocity for large clean bubbles, *J. Atmos. Ocean. Technol.*, **17**, 1392–1402.
- Leifer, I., G. de Leeuw, and L. H. Cohen (2003), Optical measurement of bubbles: System design and application, *J. Atmos. Ocean. Technol.*, **20**, 1317–1332.
- Lewis, E. R., and S. E. Schwartz (2004), *Sea Salt Aerosol Production: Mechanisms, Methods, Measurements and Models*, AGU, Washington, D. C.
- Lorenzen, C. J. (1963), Diurnal variation in photosynthetic activity of natural phytoplankton populations, *Limnol. Oceanogr.*, **8**(1), 56–62.
- Marks, R., K. Kruczalac, K. Jankowska, and M. Michalska (2001), Bacteria and fungi in air over the Gulf of Gdansk and Baltic sea, *J. Aerosol Sci.*, **32**, 237–250.
- Marra, J. (1978), Effect of short-term variations in light intensity on photosynthesis of a marine phytoplankton: A laboratory simulation study, *Mar. Biol.*, **46**, 191–202.
- Mårtensson, E. M., E. D. Nilsson, G. de Leeuw, L. H. Cohen, and H.-C. Hansson (2003), Laboratory simulations and parameterization of the primary marine aerosol production, *J. Geophys. Res.*, **108**(D9), 4297, doi:10.1029/2002JD002263.
- Mårtensson, E. M., P. Tunved, H. Korhonen, and E. D. Nilsson (2007), Submicrometre aerosol emissions from sea spray and road traffic, Ph.D. thesis, Dep. of Appl. Environ. Sci., Stockholm Univ., Stockholm.
- McNeil, C. L., B. D. Johnson, and D. M. Farmer (1995), In-situ measurement of dissolved nitrogen and oxygen in the ocean, *Deep Sea Res., Part 1*, **42**(5), 819–826.
- Medwin, H., and N. D. Breitz (1989), Ambient and transient bubble spectral densities in quiescent seas and under spilling breakers, *J. Geophys. Res.*, **94**(C9), 12,751–12,759.
- Monahan, E. C., and I. O'Muircheartaigh (1980), Optimal power-law description of oceanic whitecap coverage dependence on wind speed, *J. Phys. Oceanogr.*, **10**, 2094–2099.
- Monahan, E. C., and I. O'Muircheartaigh (1986), Whitecaps and the passive remote-sensing of the ocean surface, *Int. J. Remote Sens.*, **7**(5), 627–642.
- Murphy, D. M., J. R. Anderson, P. K. Quinn, L. M. McInnes, F. J. Brechtel, S. M. Kreidenweis, A. M. Middlebrook, M. Pósfai, D. S. Thomson, and P. R. Buseck (1998), Influence of sea-salt on aerosol radiative properties in the Southern Ocean marine boundary layer, *Nature*, **392**, 62–65.
- Nilsson, E. D., Ü. Rannik, E. Swietlicki, C. Leck, P. P. Aalto, J. Zhou, and M. Norman (2001), Turbulent aerosol fluxes over the Arctic Ocean: 2. Wind-driven sources from the sea, *J. Geophys. Res.*, **106**(D23), 32,139–32,154.
- Nilsson, E. D., E. M. Mårtensson, J. S. Van Ekeren, G. de Leeuw, M. Moerman, and C. O'Dowd (2007), Primary marine aerosol emissions: Size resolved eddy covariance measurements with estimates of sea salt and organic carbon fractions, *Atmos. Chem. Phys.*, **7**, 13,345–13,400.
- O'Dowd, C. D., and M. H. Smith (1993), Physicochemical properties of aerosols over the Northeast Atlantic: Evidence for wind-speed-related submicron sea-salt aerosol production, *J. Geophys. Res.*, **98**(D1), 1137–1149.
- O'Dowd, C. D., M. H. Smith, I. E. Consterdine, and J. A. Lowe (1997), Marine aerosol, sea-salt, and the marine sulphur cycle: A short review, *Atmos. Environ.*, **31**(1), 73–80.
- O'Dowd, C. D., M. C. Facchini, F. Cavalli, D. Ceburnis, M. Mircea, S. Decesari, S. Fuzzi, Y. J. Yoon, and J.-P. Putaud (2004), Biogenically driven organic contribution to marine aerosol, *Nature*, **431**, 676–680.
- O'Dowd, C. D., B. Langmann, S. Varghese, C. Scannell, D. Ceburnis, and M. C. Facchini (2008), A combined organic-inorganic sea-spray source function, *Geophys. Res. Lett.*, **35**, L01801, doi:10.1029/2007GL030331.
- Paterson, M. P., and K. T. Spillane (1969), Surface films and the production of sea-salt aerosol, *Q. J. R. Meteorol. Soc.*, **95**, 526–534.
- Pierce, J. R., and P. J. Adams (2006), Global evaluation of CCN formation by direct emission of sea salt and growth of ultrafine sea salt, *J. Geophys. Res.*, **111**(D6), D06203, doi:10.1029/2005JD006186.
- Reinke, N., A. Vossnacke, W. Schütz, M. K. Koch, and H. Unger (2001), Aerosol generation by bubble collapse at ocean surfaces, *Water Air Soil Pollut.*, **1**, 333–340.
- Resch, F., and G. Afeti (1992), Submicron film drop production by bubbles in seawater, *J. Geophys. Res.*, **97**(C3), 3679–3683.
- Rodríguez Niño, M. R., and J. M. Rodríguez Patino (1998), Surface tension of protein and insoluble lipids at the air-aqueous phase interface, *J. Am. Oil Chem. Soc.*, **75**, 1233–1239.
- Seinfeld, J. H., and S. N. Pandis (2006), *Atmospheric Chemistry and Physics*, John Wiley, Hoboken, N. J.

- Sellegrì, K., C. D. O'Dowd, Y. J. Yoon, S. G. Jennings, and G. de Leeuw (2006), Surfactants and submicron sea spray generation, *J. Geophys. Res.*, *111*, D22215, doi:10.1029/2005JD006658.
- Stramska, M., R. Marks, and E. C. Monahan (1990), Bubble-mediated aerosol production as a consequence of wave breaking in supersaturated (hyperoxic) seawater, *J. Geophys. Res.*, *95*(C10), 18,281–18,288.
- Thorpe, S. A. (1982), On the clouds of bubbles formed by breaking wind-waves in deep water, and their role in air-sea gas transfer, *Philos. Trans. R. Soc. London, Ser. A*, *304*(1483), 155–210.
- Tyree, C. A., V. M. Hellion, O. A. Alexandrova, and J. O. Allen (2007), Foam droplets generated from natural and artificial seawaters, *J. Geophys. Res.*, *112*, D12204, doi:10.1029/2006JD007729.
- von Glasow, R., and P. J. Crutzen (2004), Model study of multiphase DMS oxidation with a focus on halogens, *Atmos. Chem. Phys.*, *4*, 589–608.
- Wanninkhof, R. (1992), Relationship between wind speed and gas exchange over the ocean, *J. Geophys. Res.*, *97*(C5), 7373–7382.
- Weber, M. E., D. C. Blanchard, and L. D. Syzdek (1983), The mechanism of scavenging of waterborne bacteria by a rising bubble, *Limnol. Oceanogr.*, *28*(1), 101–105.
- Wotton, R. S., and T. M. Preston (2005), Surface films: Areas of water bodies that are often overlooked, *BioScience*, *55*(2), 137–145.
- Yoon, Y. J., et al. (2007), Seasonal characteristics of the physiochemical properties of North Atlantic marine atmospheric aerosol, *J. Geophys. Res.*, *112*, D04206, doi:10.1029/2005JD007044.

G. de Leeuw, Climate Change Unit, Finnish Meteorological Institute, PO Box 503, Helsinki FIN-00101, Finland.

M. Ehn, Department of Physics, University of Helsinki, PO Box 64, Helsinki FIN-00014, Finland.

Å. Hagström, Swedish Institute for the Marine Environment, Guldhedsgatan 5A, PO Box 460, Gothenburg SE-405 30, Sweden.

K. A. H. Hultin, R. Krejci, E. M. Mårtensson, and E. D. Nilsson, Department of Applied Environmental Science, Stockholm University, Stockholm SE-106 91, Sweden. (kim.hultin@itm.su.se)